

**A Comparison of One Tenth
and Full-Scale Measurements
of the Drag and Geometry of
a Pelagic Trawl**

MAFF COMMISSION

Seafish Report No. 409

**A Joint Report by:
Sea Fish Industry Authority
SOAFD Marine Laboratory**

September 1992

**MAFF R&D Commission 1991/92
© Crown Copyright 1992**

SEA FISH INDUSTRY AUTHORITY

Seafish Technology

SOAFD

Marine Laboratory

A COMPARISON OF ONE TENTH AND FULL-SCALE MEASUREMENTS OF THE DRAG AND GEOMETRY OF A PELAGIC TRAWL (MODEL-FULL SCALE CORRELATION)

Crown Copyright 1992

Seafish Report No. 409

***MAFF R&D Commission 1991/92**

Project Codes IAA16 (MAFF), GT1 (Seafish)

J N Ward (Sea Fish Industry Authority)

R S T Ferro (SOAFD Marine Laboratory)

***Sea Fish Industry Authority work carried out under MAFF R&D Commission**

SEA FISH INDUSTRY AUTHORITY

Seafish Technology

SOAFD

Marine Laboratory

Seafish Report No. 409

J N Ward (Sea Fish Industry Authority)

***MAFF R&D Commission 1991/92**

R S T Ferro (SOAFD Marine Laboratory)

Project Codes IAA16(MAFF), GT1(Seafish)

***Sea Fish Industry Authority work carried out under MAFF R&D Commission**

A COMPARISON OF ONE TENTH AND FULL-SCALE MEASUREMENTS OF THE DRAG AND GEOMETRY OF A PELAGIC TRAWL(MODEL- FULL SCALE CORRELATION)

SUMMARY

Current practices in modelling fishing gear have been investigated by comparing the shape and drag of a nylon pelagic trawl at $1/10$ scale with those of its full-scale equivalent.

Careful attention was paid to the design and manufacture of the model to ensure that the currently accepted practices based on maintaining constant Froude Number were observed.

The results show that the drag coefficient for the net may be significantly higher at model scale because constant Reynolds Number is not maintained between model and full-scale. Furthermore, considerable changes in the shape and drag of the model were observed when small changes were made to the hanging ratio of the netting on the selvedge ropes.

It is concluded that accurate modelling must take into account rope and twine elongation, particularly in nylon nets, and the change of drag coefficient with Reynolds Number when Froude Number is held constant.

**A COMPARISON OF ONE TENTH AND FULL-SCALE MEASUREMENTS
OF THE DRAG AND GEOMETRY OF A PELAGIC TRAWL**

J.N. Ward and R.S.T. Ferro*

Sea Fish Industry Authority, St Andrews Dock, Hull

***SOAFD Marine Laboratory, Aberdeen**

**Proofs to: Mr R S T Ferro, SOAFD Marine Laboratory, PO Box 101,
Victoria Road, Torry, Aberdeen AB9 8DB, UK.**

Abstract

Ward, J.N. and Ferro, R.S.T., 1992. A comparison of one tenth and full-scale measurements of the drag and geometry of a pelagic trawl. Fisheries Research.....

Current practices in modelling fishing gear have been investigated by comparing the shape and drag of a nylon pelagic trawl at $1/10$ scale with those of its full-scale equivalent.

Careful attention was paid to the design and manufacture of the model to ensure that the currently accepted practices based on maintaining constant Froude Number were observed.

The results show that the drag coefficient for the net may be significantly higher at model scale because constant Reynolds Number is not maintained between model and full-scale. Furthermore, considerable changes in the shape and drag of the model were observed when small changes were made to the hanging ratio of the netting on the selvedge ropes.

It is concluded that accurate modelling must take into account rope and twine elongation, particularly in nylon nets, and the change of drag coefficient with Reynolds Number when Froude Number is held constant.

Introduction

Since the introduction of flume tanks to test model fishing gears there has been much debate about the most suitable modelling rules to ensure that the models represent the real gears as faithfully as possible (Christensen, 1975, Dickson, 1961, Fridman, 1973, Tauti, 1934). It has

been accepted that not all requirements for accurate modelling can be fulfilled simultaneously.

Various theoretical approaches have been derived but it has not been possible to test their suitability because there has never been a comprehensive set of measurements on the same net at both full-scale and the model scales usually necessary in flume tanks or wind-tunnels.

A joint project was undertaken by the Sea Fish Industry Authority and Marine Laboratory to obtain two such sets of measurements. A pelagic trawl was chosen to avoid the complication of ground friction which is not easy to model accurately in a flume tank (Wileman, 1980).

In 1983 the Marine Laboratory obtained a set of full-scale measurements on a four panel nylon pelagic trawl (reference number PT163). The data provided estimates of net drag, overall net geometry and also mesh setting angles along the net.

A $1/10$ scale model of the net was subsequently made and tested in the SFIA flume tank in Hull, measuring a similar set of parameters for comparison with the full-scale.

This report describes the methods used to model the net accurately and compares the results of the two experiments. Observations on modelling techniques are made, particularly with regard to the effect of Reynolds Number and the modelling of extensibility.

Description of trials

The full-scale trials on trawl PT163 were conducted on the 600 hp research vessel FRV Clupea (Ferro and Hall, 1984). Careful measurements of loads and geometry of the trawl were made using underwater

instrumentation and a remote controlled underwater television vehicle in the sheltered waters of the Sound of Raasay, west of Scotland. The instruments recorded mean values over 30 second periods which themselves were averaged over periods of 5 to 15 minutes when the engine speed was held constant. Three hauls during this cruise provided comprehensive sets of measurements and were chosen for detailed analysis. During or immediately after the trials careful measurements were made of the major parameters defining the net design, such as twine thickness, mesh size, rope lengths, etc. A net drawing (Fig. 1) was then made, corresponding as nearly as possible to the net as tested.

In 1987/8, the $1/10$ scale model was built (Fig. 2). Initially it was tested with no ropes along the selvages (21 June 1988). A further brief test was done (8 February 1990) with selvedge ropes attached, using the hanging ratios measured on the full-scale net (Table I). Subsequently another set of measurements (22 April 1991) was made, lengthening the selvedge ropes in some panels to try to simulate the expected elongation of these ropes under load. Finally on the same day, the selvedge ropes were removed to check that the model was behaving as it had during the first model trials on 21 June 1988.

Basis for modelling calculations

In the UK, model nets have traditionally been constructed using constant Froude Number modelling rules (Appendix I). It was decided to build the model of PT163 as closely as possible to these rules. The main disadvantage is that the Reynolds Numbers of the model and full-scale nets will be different. Hence the flows at the two scales will not be similar. As

a consequence, the drag coefficients of basic shaped bodies such as cylinders vary and, over the range of Reynolds Numbers of interest, the drag coefficient of the whole net may also vary. This possibility is considered in the analysis of the data.

A true scale model requires that both the mesh size and twine diameter are scaled by the appropriate factor (ie 1:10 in this case), and also that the number of meshes across and along the panel are the same in the model as in the full-scale net.

Although a wide range of model mesh sizes is available, these are stocked in only three twine diameters for full mesh sizes between 10 mm and 42 mm and in two twine diameters for those above 42 mm full mesh size.

As the model twine diameters are rarely exactly the correct scale size, not all characteristics can be maintained in the model.

It is considered that the important parameters to scale correctly in the model are twine surface area, solidity, mesh angles and overall linear dimensions.

In order to model twine surface area correctly the ratio of twine diameter to mesh size should be the same for a full-scale panel and its model equivalent.

$$D/2A \text{ (full-scale)} = d/2a \text{ (model)}$$

where D = diameter of full-scale twine

$2A$ = full mesh size in full-scale net section

d = diameter of model twine

$2a$ = full mesh size of model twine

After the model twine diameter has been chosen from the limited number available, the appropriate model mesh size can be calculated.

$$2a = (2A \times d)/D$$

As this full mesh size may not be available in the model netting stock the nearest size $2a'$ is chosen.

The number of meshes across and along the section is then modified to ensure twine area and overall linear dimensions are modelled accurately.

$$n = (2A \times N)/(2a' \times \lambda)$$

where n = number of meshes across or along the model section

N = number of meshes across or along the full-scale section

$2a'$ = full mesh size in model net section

The extent to which the model of PT163 differed from the intended overall scale of 1:10 has been calculated (Table II).

The mesh scale factor is different in almost every section, varying from a value of over 13 for the forward sections to less than 4 for the cod-end sections, compared to the overall linear scale factor of 10. However, the key parameters such as solidity, twine area and section stretched length and width are usually close to the required scale. In this case the total twine area is within 0.5% of the required value for a true $1/10$ scale model.

The mesh setting angles should also be close to the full-scale values if the overall geometry of the model net is correct when tested in the tank but will clearly depend on the dimensions of the each netting section.

To assess how well extensibility is modelled, elongation has been estimated (Table II) assuming it is proportional to netting drag and inversely proportional to elastic modulus and cross-sectional area of twine across a netting section (see Appendix I). This derived scale factor for elongation is between 7 and 31 times too small, so that any elongation in the full-scale will not be reproduced in the model.

Setting up the model in the flume tank

General

At $1/10$ scale the full otterboard spread would not fit within the width of the tank and only the aft 26 m of the bridle were modelled. Consequently it was necessary to calculate the vertical and horizontal separations of the forward ends of the bridles which would give the required full-scale bridle geometry. Because the whole gear was not modelled, the horizontal spread of the fore end of the bridles had to be chosen to ensure that the wing-end spread matched the full-scale values. Furthermore, the wing-end weighting was altered as necessary to ensure that the vertical geometry was exactly as at full-scale. The net mouth geometry was therefore constrained to match the full-scale data. Checks on the accuracy of the model could thus be made only on net drag and the detailed geometry of the netting sections aft of the net mouth.

In calculating the full-scale bridle geometry, it was assumed that the wires were straight, that the vertical height between the upper and lower

wing-ends was equal to the headline height, that the upper and lower bridles were in the same vertical plane and that the otterboards were not heeled or pitched.

From Figure 3, the following equations can be derived:

$$x = L_b \cdot \cos B - L_t \cdot \cos A$$

$$l_t = (l_b \cdot \cos B - x) / \cos A \text{ or } l_b = (l_t \cdot \cos A + x) / \cos B$$

$$v_s = l_t \cdot \sin A - l_b \cdot \sin B + w_s$$

$$y_t = y_n + (l_b / L_b) \cdot (y_b - y_n)$$

where A = vertical angle of upper bridle

B = vertical angle of lower bridle

L_t = total length of upper bridle

L_b = total length of lower bridle

l_t = length of modelled upper bridles

l_b = length of modelled lower bridles

x = bridle asymmetry in plane of bridles

y_b = door spread

y_n = net spread

y_t = spread at towing points in flume tank

w_s = wing-end height

v_s = vertical separation of forward ends of bridles

Given full-scale data and having chosen the length of the upper bridles, the required length of the lower bridle, and the spread and vertical

separation of the forward end of the bridles (Table III, lines a and b) can be estimated using the expressions above.

Extensibility and flexibility

For nets made of nylon it is thought that the extensibility of the twine plays an important role in absorbing shock loads and distributing the load evenly over the netting (Klust, 1982). It is clear that the elongation of the model twine under load will be very much lower than it should be (Table II) because the elastic modulus and twine diameter are incorrectly scaled. The flexibility of the twine is also modelled inaccurately. The inadequacy of modelling cod-ends may be attributed to this exaggerated stiffness and the excess weight of the netting. The lack of elongation of the selvedge ropes may also cause errors in geometry of at least similar magnitude because this alters their effective hanging ratio.

To investigate this question the model was tested on three occasions representing three selvedge conditions. Firstly on 21 June 1988 no selvedge ropes were used so that almost all of the tension was transmitted through the netting panels. Secondly, on 8 February 1990, selvedge ropes were attached using the hanging ratios measured during the full-scale trials (Table I). In this case too much tension was taken by the selvedge ropes because they would not stretch under the model loads. Thirdly, the selvedge ropes were rerigged (22 April 1991) making allowance for the likely elongation which would have occurred in full-scale (Appendix II). A final test was done on the same day in which the selvedge ropes were removed to check that the model was behaving in the same way as in the

first trials on 21 June 1988. Despite the lapse of time there was good agreement between these two measurements.

Instrumentation and method of measurement

Bridle tensions

The four bridle loads were measured by load cells of approximately 5 kg capacity. The load cells were connected to a data logging system which measured each load every two seconds and then gave the average load every 30 seconds.

The normal method of measuring warp tensions in the Flume Tank is to attach each warp to a tow post using a fixed length of wire. The wire length is unchanged as the tow point on each tow post is lowered beneath the water surface to the required depth. A recoil mechanism pays out wire as the tow point is lowered, then the load cell is engaged on the wire by a lever mechanism.

The PT163 test required two bridle tensions to be measured on each tow post with the bridles separated vertically by a predetermined distance, v_s (Fig. 3).

A mechanism (Fig. 4) was manufactured allowing a second load cell to be mounted on each tow post. The lower bridle was attached to the existing mechanism whilst the upper bridle was attached to a new mechanism which could be set at distance v_s above the lower bridle. Because there was no recoil mechanism for the upper bridle the wire was attached to the load cell manually. This required that the tow points were firstly lowered beneath the water surface to the required depth, the lower

bridle load was then engaged by the lever after which the lower bridle load was pulled in by a predetermined distance and engaged onto the load cell.

Water speed

As the water flow in the Flume Tank varies over the section used for testing PT163, an average speed was measured over a grid of five points.

When the net was set up to the correct geometry, five speed log measurements were made in the transverse plane containing the wing-ends: three on the vertical centre-line of the net a) level with the headline centre, b) level with the footrope centre and c) at the midpoint between the other two; two further measurements at the same height as c) but in line with either wing-end. The speed was taken as the mean of the five readings.

The water speed was measured using a Braystoke water current meter attached to a pole on the Flume Tank trolley. The log impeller unit was placed at the required positions across the net, and then the impeller revolutions counted electronically over a period of 50 seconds. The rate of impeller rotation was then calculated and speed obtained from the log calibration chart.

Model Geometry

The wing-end height and bridle vertical angles were measured with reference to the water surface (Fig. 5).

The distance v_s and distance of the lower bridle below the water surface were fixed before starting the experiment.

The distances of the wings beneath the water surface were measured by sighting the level on a calibrated pole lowered from the Flume Tank trolley.

These measurements (Fig. 5) were then used to calculate the wing-end height and bridle vertical angles.

Horizontal wing-end spread was measured by sighting each wing from a horizontal scale attached to the Flume Tank trolley.

Mesh setting angles were measured using video cameras, one viewing vertically down from the trolley and one horizontally through the windows.

A small area of the white polyamide netting was coloured in each panel to be measured, allowing easy identification and also to facilitate focusing of the cameras. The coloured area was midway along each section to avoid areas of distorted meshes near the joining rounds. The angles were measured manually on the video monitors, taking an average over several meshes in each case and allowing for distortion and scaling on the screen as necessary.

Results

The full-scale trials provided detailed measurements on three hauls over a range of speeds from 3.35 to 3.69 knots (Table IV).

The main parameters for assessing the accuracy of the modelling technique are the loads in the bridles, the net drag and the mesh angles in the netting sections along the top and side panels of the net. The model results have been converted to full-scale values for ease of comparison; model speed has been multiplied by the square root of the scale and the forces by the cube of the scale.

As has already been mentioned, the model bridle geometry and net mouth are both constrained to match the full-scale values and cannot be used to assess the model accuracy.

The distances between the upper and lower panels and between the side panels at each netting section join were also measured in the tank and by echosounder at full-scale but meaningful comparisons could not be made because of the lack of discrimination of the echosounder over short distances.

Bridle tensions and net drag

The ratio of the upper and lower bridle tensions (Table IV) is determined by the relative lengths of the upper and lower bridles.

The upper bridle tensions are consistently higher than the lower bridle tensions for both models with no selvedge ropes (21 June 1988 and 22 April 1991). There is however, some variation in their ratios (Column 4). This ratio is very sensitive to the precision with which the bridle lengths are set up at the towing posts. In haul 273 on 22 April 1991, the tension ratio seems to be high.

The full-scale values are however, in the range covered by the model results. This suggests that the net is rigged correctly in the tank despite the sensitivity due to the method of setting up the bridles.

The net drags have been expressed as percentages of the values for the full-scale net and also corrected for small differences in speed by multiplying by the ratio of the square of the speeds. The drags for the nets with no selvedge ropes are consistently high compared to the full-scale drags. They vary from 9 to 26% higher.

There is however, a major change when the selvedge ropes are attached (model 22 April 1991 with rope). The ropes take the load from the netting which then become slacker allowing the meshes to open and the net diameter at a given cross-section to expand. The profile of the net therefore changes from a trumpet shape to one in which the netting is straight or even balloons outwards to some extent. The total net drag increases from about 17% higher to about 61% higher than full-scale drag. The increased angle of attack of the twines to the water flow is a likely cause of the increase in drag. This effect of hanging ratio on drag is likely to be greater than that due to twine area modelling inaccuracies and may be of the same order, or larger than, any Reynolds Number effect.

Mesh angles

The mesh setting angles were measured in five sections of the top panel and port side panel of both the full-scale and the three model cases. The equivalent hanging ratios of the netting on the selvedge ropes for each case are given in Table I.

The mesh angle data are consistent (Table V); for instance, the mean absolute difference in mesh angles between the two 'no rope' data sets is only 11%, over all sections. Furthermore, the measured angles for the three hauls are similar, the differences in speed and mouth geometry having no major effect. To simplify analysis the mean values for the three hauls have been calculated (Table VI) and will be referred to in the discussion. The results for the two 'no rope' cases have also been averaged.

a) Top panel

It can be seen that the mesh angles in the top panel of the full-scale net reduce gradually along the length of the net. This typical configuration is borne out by many years' observations of trawls during fishing.

There is no corresponding gradual reduction in mesh angle along the top panel of the model nets. While the angles in sections B and C are in good agreement, the model angles for sections D-F tend to increase towards the aft end, the smaller the hanging ratio the greater the mesh angles. These results suggest that the hanging ratios for the case with the allowance for elongation of the selvedge rope (Line 3) are nearly the required values. A lower hanging ratio is required in section D and a higher one in section F. The sharp increase in angle for section F as the selvedge rope is shortened may be partly due to the poor modelling of the stiffness, weight and drag of sections G-K further aft (Fig. 2).

b) Side panels

The side panels were not opened fully because during the full-scale trials the wing-end weights were chosen to be smaller than normal to ensure the net fished at depths shallow enough for good visibility. The angles for section B are uncertain because of the consequent distortion of this section. The side panel mesh angles tend to be in a narrower range of values.

Nevertheless the full-scale mesh angles reduce gradually along the net whereas, in the models, there are abrupt changes in angle from one section to the next, suggesting that the geometries of neighbouring sections may be independent and that load may not be transmitted uniformly along the net.

This variability may be explained by the low loading in the side panel because it is not opened properly.

Discussion

Without selvedge ropes the model mesh angles are too low (Table VI) in most sections, particularly in the top panel. It would therefore be expected that the drag, which increases with mesh angle, might be too low in the 'no rope' case. There is however, an increase in drag of about 17%. This may indicate a Reynolds number effect.

At full-scale the Reynolds Number is 5020 (1.8 m/s, 4.1 mm twine, viscosity of 1.47×10^{-6} m²/s) compared to 149 for the model (0.57 m/s, 0.3 mm twine and viscosity of 1.15×10^{-6} m²/s). From the appropriate ESDU data sheet (Anon., 1980), assuming that the roughness factor is similar for model and full-scale, the drag coefficient is 1.00 and 1.35 respectively at these Reynolds Numbers for a circular cylinder normal to the flow. The observed 17% increase in drag mentioned above would be consistent with these figures if the mesh angle change caused an 18% reduction in drag. This reduction seems reasonable.

Changing the proportion of load taken by the netting and by the selvedges has a major effect on net drag because of the change in orientation of the mesh bars to the flow. When the selvedge ropes are attached with an allowance for elongation, the model mesh angles generally become larger. The model drag is seen to be approximately 61% greater than at full-scale. Deducting the 35% due to Reynolds Number effect gives an increase of 26% due to the change in mesh angles. It may be that the allowance for elongation was somewhat too large at least for some of the

netting sections. These estimates do little more than confirm that differences in drag due to mesh angle and to change in Reynolds Number are a plausible explanation of the results; they may not be the correct explanation.

Clearly however, the model shape and drag are sensitive to selvedge hanging ratios. The problem for the model builder is that the ropes will suddenly start to take tension when their length is reduced below a critical length (the netting length when towing). Hence if nets are designed with hanging ratios close to this condition it is difficult to achieve the correct model shape. The problem is made worse as there is no accurate method of estimating the load and hence the elongation of the model ropes whose extensibility is not modelled correctly. The sensitivity is shown in section D (Table VI) where the model rope seems too long for the top panel (angles too small) but too short for the side panel (angles too large). This discrepancy could also be explained if the mesh size measurement in section D in either the top or side panel was incorrect.

Finally in the case where the ropes are attached without allowance for elongation (trials on 8 February 1990), the hanging ratios are changed significantly again. Only in section F however, is there significant change in mesh angle (Table VI), suggesting that in the other sections the selvedge ropes were already taking the maximum proportion of net drag and allowing the netting to be very slack. No drag measurements were made in this case.

Conclusions

Careful design and planning is needed to build a model net which is to behave in a similar way to a full-scale net. All model materials should be measured carefully beforehand so that the correct selection of twine and mesh size can be made for each netting section. If a known full-scale net is being modelled then a complete set of measurements of its dimensions and materials should also be made, including mesh size, twine diameter (Ferro, 1989), meshes in each section, wire and rope lengths and diameters, hanging ratios and weighting and flotation around the net mouth. Use of the modelling techniques outlined in this report should ensure that discrepancies between model and full-scale results should not arise due to inadequate similarity in twine area, solidity and geometric dimensions.

Two additional sources of error in simulating drag have been identified. Firstly, if model speed is chosen according to Froude scaling laws then the Reynolds Number will not be correct so that the ratio of the inertial and viscous forces acting on the model will not be equal to that for the full-scale net. There is a significant difference between model and full-scale Reynolds Number for the twine. Standard data sheets indicate that this would cause an increase of the order of 35% in the drag coefficient of a rigid cylinder. Secondly, the hanging ratio of the netting on the selvedge ropes has been found to have a critical effect on the shape of individual netting sections. When the selvedge ropes are too short they take too much of the load. Thus the netting is slack, the net diameter increases, the mesh bars take up larger angles to the flow and the drag is increased. The opposite occurs when the ropes are too long.

These experiments suggest that, after allowance for a possible Reynolds Number effect, model drag was underestimated by about 18% when hanging ratio was overestimated (case without ropes). Similarly the drag was estimated to be too large by about 26% when hanging ratios were too small (case with ropes and elongation allowance).

It would require hanging ratios of perhaps 0.95, 0.9 and 0.95 for the selvedge ropes along sections D, E and F in order to achieve closer similarity in drag. It might also be necessary to model the sections towards the aft end of the net, from section F, more accurately in terms of weight, extensibility and flexibility. In this way the shape of, and flow through the aft sections and cod-end would be more realistic.

Methods to quantify these two major sources of error independently are needed. It would be possible to compare a model and full-scale net made of twine and ropes with little or no elongation. Polyester (PES) may be more suitable, for instance. This would allow a study of the Reynolds Number effect alone. Having established the Reynolds Number effect, a more rigorous investigation of the effect of elongation could be undertaken.

Acknowledgements

The authors are grateful to all members of the SFIA Industrial Development Unit and of the SOAFD Marine Laboratory who helped in the full-scale and model trials - in particular Adrian Strickland of SFIA and Chris Hall of SOAFD.

References

- Anon., 1980. ESDU Data Sheet 80025. Mean forces, pressures and flow field velocities for circular cylindrical structures. Engineering Sciences Data Unit, London, 55pp.
- Christensen, B.A., 1975. Hydrodynamic modelling of fishing nets. In: Proceedings of Ocean 75 Conference, IEEE: 484-490.
- Dickson, W., 1961. Trawl performance. A study relating model to commercial trawls. DAFS Marine Research 1. HMSO, Edinburgh, 48 pp.
- Ferro, R.S.T., 1989. Objective measurement of the thickness of netting twine used in the fishing industry. Fisheries Research, 8: 103-112.
- Ferro, R.S.T. and Hall, C.D., 1984. Full-scale measurements of the geometry and loading of a four panel nylon pelagic trawl (PT163). Scottish Fisheries Working Paper 4/84 (unpubl.), 19 pp.
- Fridman, A.L., 1973. Theory and design of commercial fishing gear. Israel program for scientific translations. National Marine Fisheries Service, 489 pp.
- Klust, G., 1982. Netting materials for fishing gear. Fishing News Books Ltd, Osney Mead, Oxford, UK, 175 pp.
- Klust, G., 1983. Fibre ropes for fishing gear. Fishing News Books Ltd, Osney Mead, Oxford, UK, 199 pp.
- Reid, A.J., 1977. A net drag formula for pelagic nets. Scottish Fisheries Research Report 7, 12pp.
- Tauti, M., 1934. A relation between experiments on a model and a full-scale fishing net. Bulletin of Japanese Society of Scientific Fisheries 3(1): 171-177.

Wileman, D.A., 1980. Problems encountered in the correlation between the results of engineering performance trials of full scale trawls at sea and scaled modeltrawls tested in the White Fish Authority flume tank, Hull. WFA Field Report 857, 30 pp.

Table I

Schedule of tests and the hanging ratios of the netting on the selvages of each section of netting

| Test | Section | | | | |
|--|---------|------|------|------|------|
| | B | C | D | E | F |
| Full-scale (measured) | 0.98 | 0.87 | 0.90 | 0.83 | 0.84 |
| Model 21.6.88 No rope) | 1 | 1 | 1 | 1 | 1 |
| Model 22.4.91 No rope) | | | | | |
| Model 22.4.91 With rope and elongation allowance | 1 | 1 | 1 | 0.90 | 0.88 |
| Model 8.2.90 With rope but no elongation allowance | 0.98 | 0.87 | 0.90 | 0.83 | 0.84 |

Table II

Scale factors (full-scale/model scale) for major parameters in each individual netting section in the top and side panels. The top line indicates the target scale factors to be achieved if modelled with constant Froude Number at a linear scale of 1:10

| Section | Mesh size | Twine thickness | No of rows long | No of meshes wide | Twine area | Solidity | Length | Width | Weight | Surface area | Elongation |
|---------------------------|-----------|-----------------|-----------------|-------------------|------------|----------|--------|-------|--------|--------------|------------|
| Top panel | | | | | | | | | | | |
| Target scale factors | | | | | | | | | | | |
| | 10 | 10 | 1 | 1 | 100 | 1 | 10 | 10 | 1000 | 100 | 1 |
| Actual scale factors used | | | | | | | | | | | |
| A | 13.2 | 13.7 | 0.77 | 0.72 | 102 | 1.04 | 10.2 | 9.6 | 1374 | 97 | 7.4 |
| B | 13.2 | 13.7 | 0.78 | 0.77 | 108 | 1.04 | 10.3 | 10.1 | 1488 | 105 | 7.5 |
| C | 7.6 | 7.33 | 1.36 | 1.33 | 101 | 0.97 | 10.4 | 10.1 | 739 | 104 | 14.1 |
| D | 8.3 | 8.0 | 1.19 | 1.21 | 96 | 0.95 | 9.9 | 10.0 | 765 | 99 | 12.3 |
| E | 6.73 | 6.67 | 1.47 | 1.47 | 97 | 1.0 | 9.9 | 9.9 | 647 | 98 | 14.8 |
| F | 5.02 | 5.0 | 1.99 | 2.0 | 100 | 0.99 | 10.0 | 10.0 | 499 | 100 | 20.0 |
| G | 5.02 | 5.0 | 2.0 | 2.0 | 100 | 0.99 | 10.0 | 10.0 | 502 | 101 | 20.1 |
| H | 3.9 | 4.33 | 2.57 | 2.59 | 111 | 1.11 | 10.0 | 10.1 | 487 | 101 | 23.1 |
| I | 4.2 | 4.05 | 2.38 | 2.41 | 98 | 0.96 | 10.0 | 10.1 | 395 | 101 | 24.7 |
| J | 3.65 | 3.33 | 2.77 | 2.71 | 91 | 0.91 | 10.0 | 9.9 | 304 | 100 | 30.4 |
| K | 3.8 | 3.78 | 2.64 | 2.71 | 104 | 0.99 | 10.0 | 10.3 | 388 | 103 | 26.5 |

| Section | Mesh size | Twine thickness | No of rows long | No of meshes wide | Twine area | Solidity | Length | Width | Weight | Surface area | Elongation |
|----------------------------------|-----------|-----------------|-----------------|-------------------|------------|----------|--------|-------|--------|--------------|------------|
| Side panel | | | | | | | | | | | |
| Target scale factors | | | | | | | | | | | |
| | 10 | 10 | 1 | 1 | 100 | 1 | 10 | 10 | 1000 | 100 | 1 |
| Actual scale factors used | | | | | | | | | | | |
| A | 13.3 | 13.7 | 0.77 | 0.72 | 102 | 1.04 | 10.2 | 9.6 | 1374 | 98 | 7.5 |
| B | 13.3 | 13.7 | 0.78 | 0.76 | 102 | 1.02 | 9.8 | 10.1 | 1480 | 105 | 7.6 |
| C | 7.55 | 7.33 | 1.36 | 1.32 | 99 | 0.97 | 10.3 | 10.0 | 728 | 102 | 14.0 |
| D | 6.83 | 6.67 | 1.47 | 1.50 | 100 | 0.98 | 10.0 | 10.2 | 670 | 103 | 15.1 |
| E | 6.7 | 6.67 | 1.47 | 1.49 | 97 | 1.0 | 9.9 | 10.0 | 653 | 98 | 14.8 |
| F | 4.6 | 4.33 | 2.17 | 2.18 | 95 | 0.94 | 10.0 | 10.0 | 408 | 100 | 23.1 |
| G | 4.6 | 4.33 | 2.0 | 1.96 | 78 | 0.94 | 9.2 | 9.0 | 338 | 83 | 21.2 |
| H | 3.9 | 4.33 | 2.57 | 2.59 | 110 | 1.11 | 10.0 | 10.1 | 487 | 101 | 23.1 |
| I | 4.2 | 4.05 | 2.38 | 2.42 | 97 | 0.96 | 10.0 | 10.2 | 397 | 102 | 24.7 |
| J | 3.65 | 3.33 | 2.77 | 2.75 | 92 | 0.91 | 10.0 | 10.0 | 308 | 101 | 30.4 |
| K | 3.8 | 3.78 | 2.64 | 3.0 | 114 | 1.0 | 10.0 | 11.4 | 430 | 114 | 26.5 |

Table III

Comparison of measured dimensions of the bridle system and mouth at full-scale at sea and model scale in the flume tank. The model dimensions (not angles) are converted to their full-scale equivalents by multiplying by 10

| Haul | Upper bridle length (m) | Lower bridle length (m) | Wing-end height (m) | Fore end spread (m) | Net spread (m) | Vertical separation of bridles (m) | Angles (degs) | | | |
|------|-------------------------|-------------------------|---------------------|---------------------|----------------|------------------------------------|---------------|-----|-----|------|
| | | | | | | | A | B | C | |
| 272 | a | 60.25 | 60.75 | 8.7 | 53 | 17.4 | - | 1.9 | 7.6 | 17.2 |
| | b | 25.7 | 26.0 | | 32.6 | | 6.12 | 2.2 | 7.7 | 17.4 |
| | c | 25.7 | 26.0 | 8.7 | 32.8 | 17.4 | 6.17 | 3.1 | 8.5 | 17.5 |
| | d | 25.7 | 26.0 | 8.61 | 32.95 | 17.5 | 6.17 | 2.7 | 8.4 | 15.5 |
| | e | 25.7 | 26.0 | 8.77 | 31.1 | 17.4 | 6.17 | | | |
| 273 | a | 60.25 | 60.75 | 8.0 | 58.7 | 18.4 | - | 1.4 | 6.5 | 19.5 |
| | b | 25.7 | 26.0 | | 35.6 | | 5.68 | 1.5 | 6.5 | 19.9 |
| | c | 25.7 | 26.0 | 8.0 | 36.0 | 18.5 | 5.66 | 3.1 | 8.4 | 19.4 |
| | d | 25.7 | 26.0 | 8.0 | 35.5 | 18.4 | 5.66 | 2.4 | 7.8 | 16.9 |
| | e | 25.7 | 26.0 | 8.1 | 30.2 | 18.3 | 5.66 | | | |
| 274 | a | 60.25 | 60.75 | 6.5 | 65.8 | 18.7 | - | 2.7 | 6.4 | 23.0 |
| | b | 25.7 | 26.0 | | 38.9 | | 4.81 | 3.6 | 6.8 | 21.4 |
| | c | 25.7 | 26.0 | 6.4 | 38.0 | 19.2 | 4.9 | 3.5 | 7.2 | 22.6 |
| | d | 25.7 | 26.0 | 6.6 | 39.2 | 19.4 | 4.9 | 2.6 | 6.1 | 20.5 |
| | e | 25.7 | 26.0 | 6.5 | 37.6 | 19.3 | 4.9 | | | |

Line a - full-scale values; Line b - calculated equivalent values with shortened bridles; Line c - values from tests on model with no rope (21.6.88); Line d - values from tests on model with no rope (22.4.91); Line e - values from tests on model with selvage rope (22.4.91)

See Figure 3 for definition of quantities.

Table IV

Bridle tensions and net drag for the model and full-scale nets. Net drag is calculated using the bridle angles given in Table III. Model values are converted to full-scale (see text)

| Test | Speed (knot) | 2 x Upper bridle (tonne) | 2 x Lower bridle (tonne) | Ratio U/L | Net drag (tonne) | Net drag as % of full-scale | |
|----------------------------|-----------------|-----------------------------------|-----------------------------------|--------------|------------------------|--------------------------------|----------------------------------|
| | | | | | | as measured | scaled to full-scale speed |
| Haul 272 | | | | | | | |
| Full-scale | 3.35 | 1.020 | 0.980 | 1.041 | 1.902 | 100 | 100 |
| Model 21.6.88 No rope | 3.25 | 1.146 | 1.130 | 1.014 | 2.161 | 114 | 121 |
| Model 22.4.91 No rope | 3.36 | 1.292 | 1.147 | 1.126 | 2.312 | 122 | 121 |
| Model 22.4.91 With rope | 3.34 | 1.740 | 1.588 | 1.096 | 3.189 | 168 | 169 |
| Haul 273 | | | | | | | |
| Full-scale | 3.45 | 1.100 | 1.050 | 1.048 | 2.02 | 100 | 100 |
| Model 21.6.88 No rope | 3.42 | 1.340 | 1.322 | 1.014 | 2.495 | 124 | 126 |
| Model 22.4.91 No rope | 3.51 | 1.571 | 1.055 | 1.489 | 2.464 | 122 | 118 |
| Model 22.4.91 With rope | 3.49 | 2.057 | 1.465 | 1.404 | 3.355 | 166 | 162 |
| Haul 274 | | | | | | | |
| Full-scale | 3.69 | 1.420 | 1.210 | 1.174 | 2.413 | 100 | 100 |
| Model 21.6.88 No rope | 3.75 | 1.556 | 1.384 | 1.124 | 2.725 | 113 | 109 |
| Model 22.4.91 No rope | 3.74 | 1.638 | 1.323 | 1.238 | 2.721 | 113 | 110 |
| Model 22.4.91 With rope | 3.73 | 2.238 | 1.742 | 1.285 | 3.717 | 154 | 151 |

Table V

Average mesh angles in degrees for the first five netting sections in the main body of the model and full-scale nets

| Test | Mean mesh angles in each section | | | | |
|--|----------------------------------|------|------|------|------|
| | B | C | D | E | F |
| Haul 272 - top panel | | | | | |
| Full-scale | 69? | 53 | 40 | 36.5 | 34 |
| Model 21.6.88 No rope | 59.5 | 57 | 22 | 22 | 25.5 |
| Model 22.4.91 No rope | 64 | 53 | 20 | 20 | 32 |
| Model 22.4.91 With rope | 60 | - | 32 | 46 | 64 |
| Model 2.90 With rope but no elongation allowance | 61 | 57 | 34 | 41 | 85 |
| Haul 272 - side panel | | | | | |
| Full-scale | 36? | 32 | 28.5 | 30 | 31.5 |
| Model 21.6.88 No rope | 47? | 28.5 | 41.5 | 28.5 | 23.5 |
| Model 22.4.91 No rope | - | 28 | 38 | 32 | 25 |
| Model 22.4.91 With rope | - | 36 | 57 | 52 | 62 |
| Model 2.90 With rope but no elongation allowance | - | 36 | 60 | 52 | 85 |
| Haul 273 - top panel | | | | | |
| Full-scale | - | - | - | - | - |
| Model 21.6.88 No rope | 58.5 | 56 | 23 | 23 | 27 |
| Model 22.4.91 No rope | 62 | 52 | 20 | 18 | - |
| Model 22.4.91 With rope | 60 | 59 | 34 | 40 | 61 |
| Haul 273 - side panel | | | | | |
| Full-scale | 28? | 35? | 25 | 27.5 | 29 |
| Model 21.6.88 No rope | 67.5 | 27.5 | 44 | 29 | 23.5 |
| Model 22.4.91 No rope | - | 30 | 38 | 33 | 23 |
| Model 22.4.91 With rope | - | 36 | 56 | 49 | 58 |

| Test | Mean mesh angles in each section | | | | |
|------------------------------|----------------------------------|------|------|----|------|
| | B | C | D | E | F |
| Haul 274 - top panel | | | | | |
| Full-scale | 58? | 50.5 | 42.5 | 39 | 37 |
| Model 21.6.88 No rope | 59.5 | 56.5 | 24 | 25 | 25.5 |
| Model 22.4.91 No rope | 59 | 50 | 22 | 18 | 29 |
| Model 22.4.91 With rope | 59 | 62 | 32 | 41 | 60 |
| Haul 274 - side panel | | | | | |
| Full-scale | - | 38.5 | 32.5 | 27 | 21 |
| Model 21.6.88 No rope | - | 29.5 | 39? | 30 | 22 |
| Model 22.4.91 No rope | - | 31 | 40 | 32 | 21 |
| Model 22.4.91 With rope | - | 40 | 56 | 44 | 54 |

Table VI

Summary of mesh angles in degrees averaged over the three hauls. A question mark indicates that the values are doubtful. Net drags averaged from Table IV

| Test | Mean mesh angles in each section | | | | | Net drag as % of full-scale |
|---|----------------------------------|-----|----|----|----|-----------------------------|
| | B | C | D | E | F | |
| Top panel | | | | | | |
| Full-scale | 64 | 52 | 41 | 38 | 36 | 100 |
| Model with no rope | 60 | 54 | 22 | 23 | 28 | 117 |
| Model with rope and elongation allowance | 60 | 60 | 33 | 42 | 62 | 161 |
| Model with rope but no elongation allowance | 61 | 57 | 34 | 41 | 85 | - |
| Side panel | | | | | | |
| Full-scale | 32? | 35? | 29 | 28 | 27 | 100 |
| Model with no rope | 57? | 29 | 40 | 31 | 23 | 117 |
| Model with rope and elongation allowance | - | 37 | 56 | 48 | 58 | 161 |
| Model with rope but no elongation allowance | - | 36 | 60 | 52 | 85 | - |

Appendix I

In order to achieve similarity between the model and full-scale nets it is necessary at least that the ratio of the principal forces acting on them should be the same in both cases. Classical theory proposes that this condition is achieved when the flow regime round a rigid body is similar at model and full-scale.

The Reynolds Number, R , represents the ratio between the dynamic (sometimes called inertial) forces and the viscous forces.

$$R = \frac{\rho l^2 V^2}{\mu l V} = \frac{l V}{\nu}$$

where ρ is the density of the medium, l a characteristic length, V the towing speed, μ the dynamic viscosity and the ν kinematic viscosity.

When fluids of similar kinematic viscosity are used at model and full-scale, Reynolds Number can be maintained constant only if a higher velocity is used for a smaller model size. This is impractical and models of fishing gears are rarely tested at constant Reynolds Number.

Froude Number, F , is the ratio between the dynamic forces and the gravity forces.

$$\frac{\rho l^2 V^2}{\rho g l^3} = \frac{V^2}{g l}$$

where g is acceleration due to gravity.

If Froude Number is to be kept constant then it necessarily follows that a smaller scale model must be towed at a lower speed.

It is not clear what the characteristic length should be. Dickson (1961) has argued that an overall dimension of the net should be chosen as the characteristic length and hence the velocity scaled as the root of the overall scale. This rule has been adopted at several flume tanks in Europe and has therefore been followed for this work. Other workers (eg Fridman, 1973) however, have proposed that twine diameter is the appropriate dimension.

It has been common practice, with an overall scale λ , to choose a convenient scale ratio for the mesh size and twine diameter of λ_m say (where $\lambda_m > \lambda$), to ensure that the model twines required are large enough to be practical and available. The numbers of meshes across and along each netting section are then scaled by λ/λ_m such that the projected twine area and twine surface area are scaled according to the overall scale squared, λ^2 .

The key parameters describing a section of model netting will then be scaled by the following ratios:

| Parameter | Expression | Actual scale factor | True Froude scale factor |
|---|---------------------------|-----------------------|--------------------------|
| Towing speed | $= V$ | $\lambda^{1/2}$ | $\lambda^{1/2}$ |
| Twine thickness | $= d$ | λ_m | λ |
| Mesh size | $= 2 a$ | λ_m | λ |
| Number of meshes across section | $= n$ | λ/λ_m | 1 |
| Number of meshes along section | $= r$ | λ/λ_m | 1 |
| Overall section dimensions | $\propto a n$ | λ | λ |
| Nominal twine area in section | $= 4 a d n r$ | λ^2 | λ^2 |
| Nominal weight of netting in air | $= \pi a d^{**2} n r$ | $\lambda^2 \lambda_m$ | λ^3 |
| Netting surface area | $\propto a^{**2} n r$ | λ^2 | λ^2 |
| Netting drag | $\propto a d V^{**2} n r$ | λ^3 | λ^3 |
| Cross-sectional area of twine in section | $\propto d^{**2} n$ | $\lambda \lambda_m$ | λ^2 |
| Elongation of twine \propto drag/(Elastic modulus.X sectional area) | $\propto a V^{**2} r / d$ | λ/λ_m | 1 |
| Solidity | $= d / a$ | 1 | 1 |
| Setting angle of meshes | | 1 | 1 |
| Angle of netting to flow | | 1 | 1 |

No allowance is made here for knots. In calculating elongation the elastic modulus is assumed constant for model and full-scale netting.

It can be seen that many of these key parameters determining the forces acting on the net are modelled correctly according to the overall scale λ : twine area, solidity, setting angle, angle of netting to flow and net surface area, for example.

On the other hand, there are some exceptions. When $\lambda_m > \lambda$, the twine cross-sectional area across a panel of netting is too large by a factor λ_m/λ .

If the same material is used at model and full-scale, the elastic modulus of the model twine is not scaled correctly ie the model twines will not stretch under the small loads generated in the model. If significant elongation of twines or selvedge ropes occurs at full-scale there is likely to be significant error in model net geometry.

The weight of twine in the model is also incorrect. If we assume it has the same density as the full-scale twine then it is scaled as $\lambda^2\lambda_m$ rather than λ^3 . The effect of this error may be small for most of the net since twine material density is not likely to be more than 10% different from the water density. In the sections towards the cod-end however, the hydrodynamic forces are low and the weight may be relatively large, so that the effect may be significant. For instance, in netting section J (Table II) the model twine weight in air is over three times the value according to constant Froude Number scaling. Wileman (1980) suggests cod-ends should be modelled to achieve the correct scaling of weight rather than twine area.

The aim of the experiments described in this report is to model the net precisely according to these rules and to investigate the effect of the consequent scaling errors.

Appendix II

Estimation of selvedge rope lengths under tension.

It is first necessary to estimate the load in each selvedge rope. From unpublished data, measurements of the drag of the aft end of the full-scale PT163 net are available, as well as for the complete net.

Drag of complete PT163 at 3.5 knots = 2100 kg

Drag of extension and cod-end of PT163 at 3.5 knots = 322 kg

Hence, assuming initially that the four selvedges are equally loaded and take all the drag, selvedge rope tension varies from approximately 525 to 80 kg along the net from the square to the start of the extension, section G.

The selvedge ropes are 12 mm round braided continuous filament nylon with linear density of 8.1 kg/100 m and breaking strength of 2475 kg. (Klust, 1983, Table 13).

Hence selvedge tension is in the range from 21% to 3% of breaking load.

From Klust again, this gives elongations from approximately 21% to 6% of natural length. These are high values as in practice the selvedge ropes will not take all the drag. If 67% of the drag is taken by the selvedge then the elongations become 14% to 4% from section B to F. The equivalent true selvedge lengths to be used in the model for these sections are given in the table.

| Section | B | C | D | E | F |
|---|-----|-----|-----|----|----|
| Measured natural length as % of stretched netting on actual PT163 net | 98 | 87 | 90 | 83 | 84 |
| Allowance for elongation | 14 | 12 | 10 | 7 | 4 |
| Actual rope length to be used in model as % of stretched netting | 100 | 100 | 100 | 90 | 88 |

The actual rope lengths for sections B and C are taken to be no more than 100% of the stretched netting length.

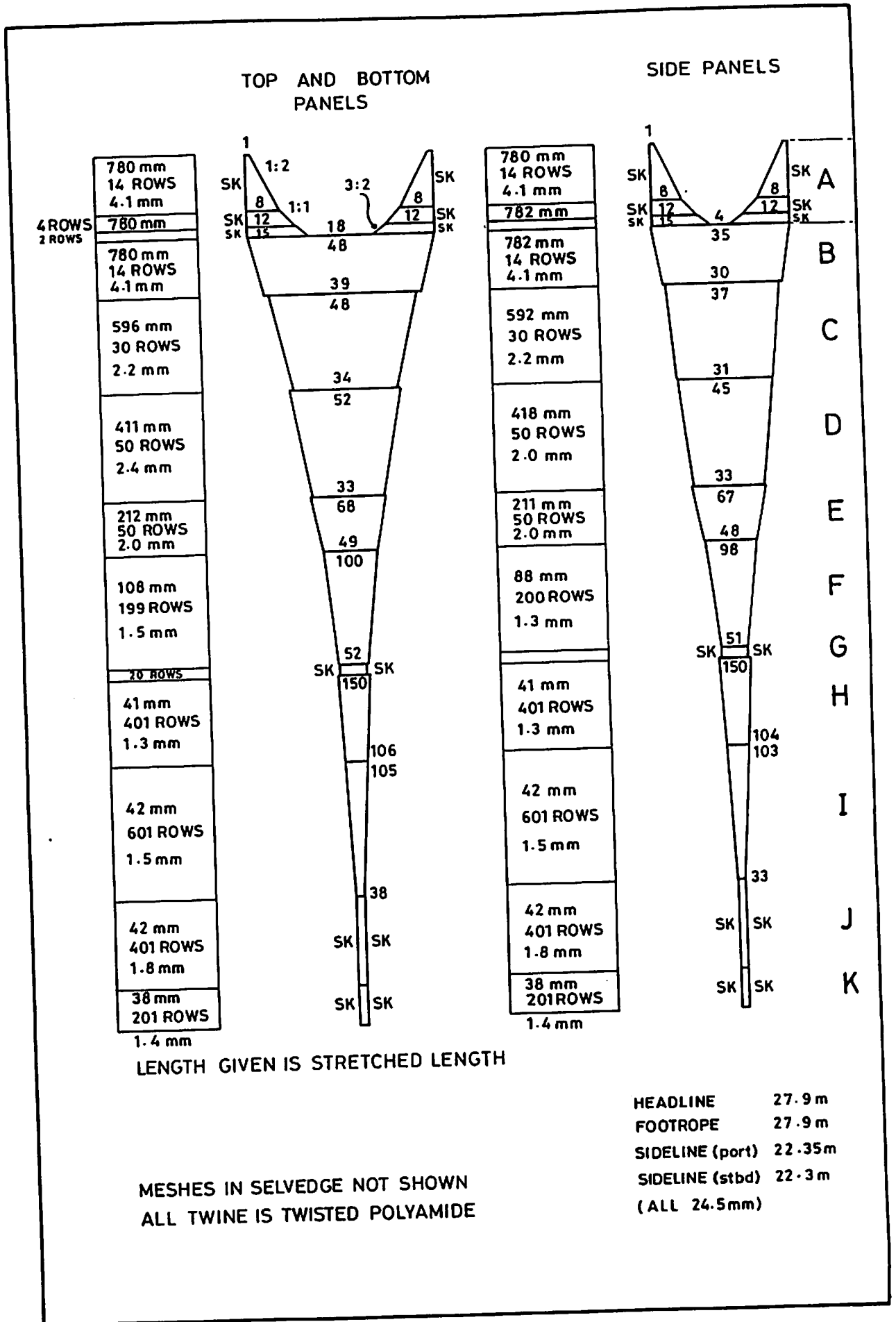


Fig.1

FULL SCALE VERSION OF PT 163 TRAWL

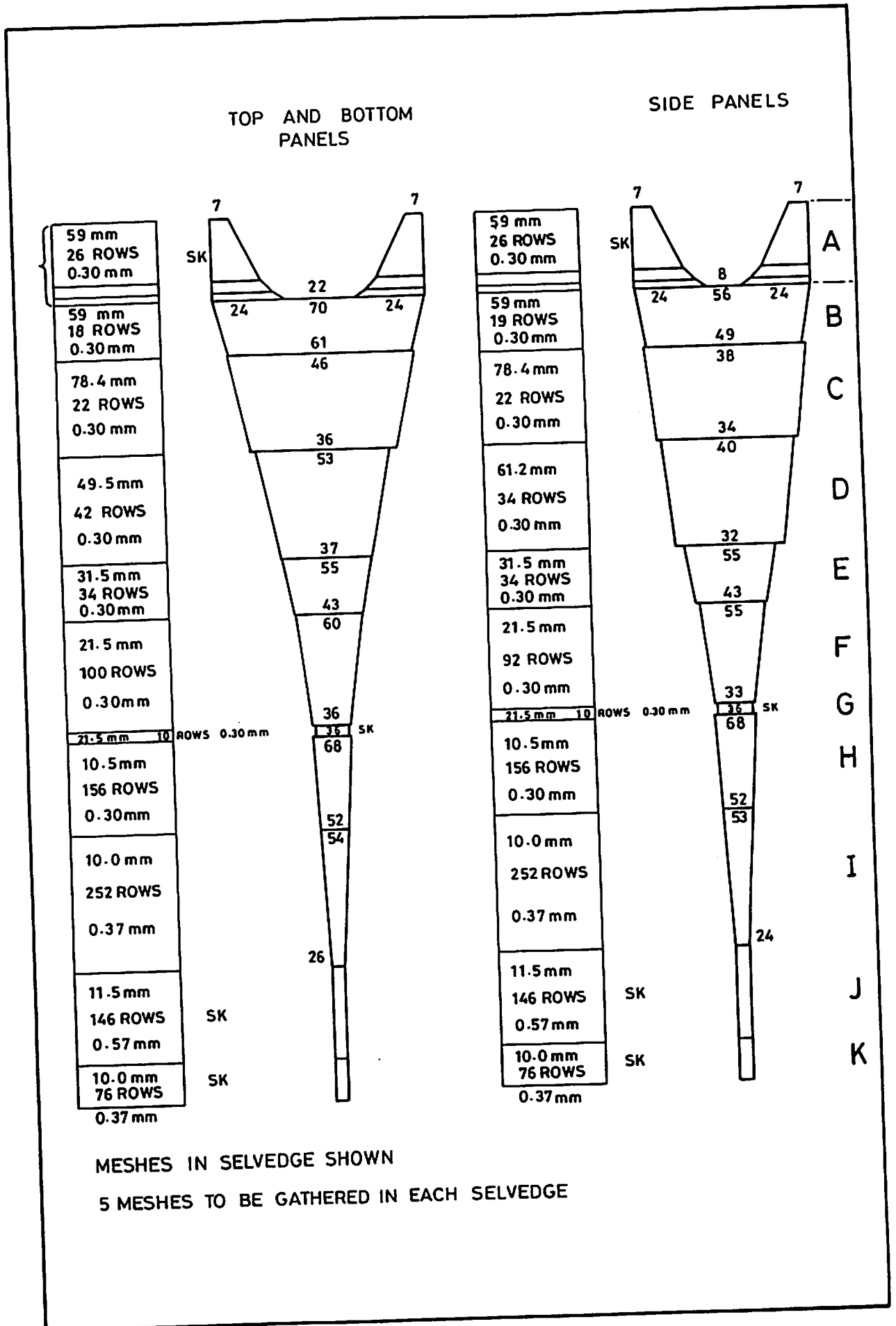


Fig.2

MODEL VERSION OF PT163 TRAWL

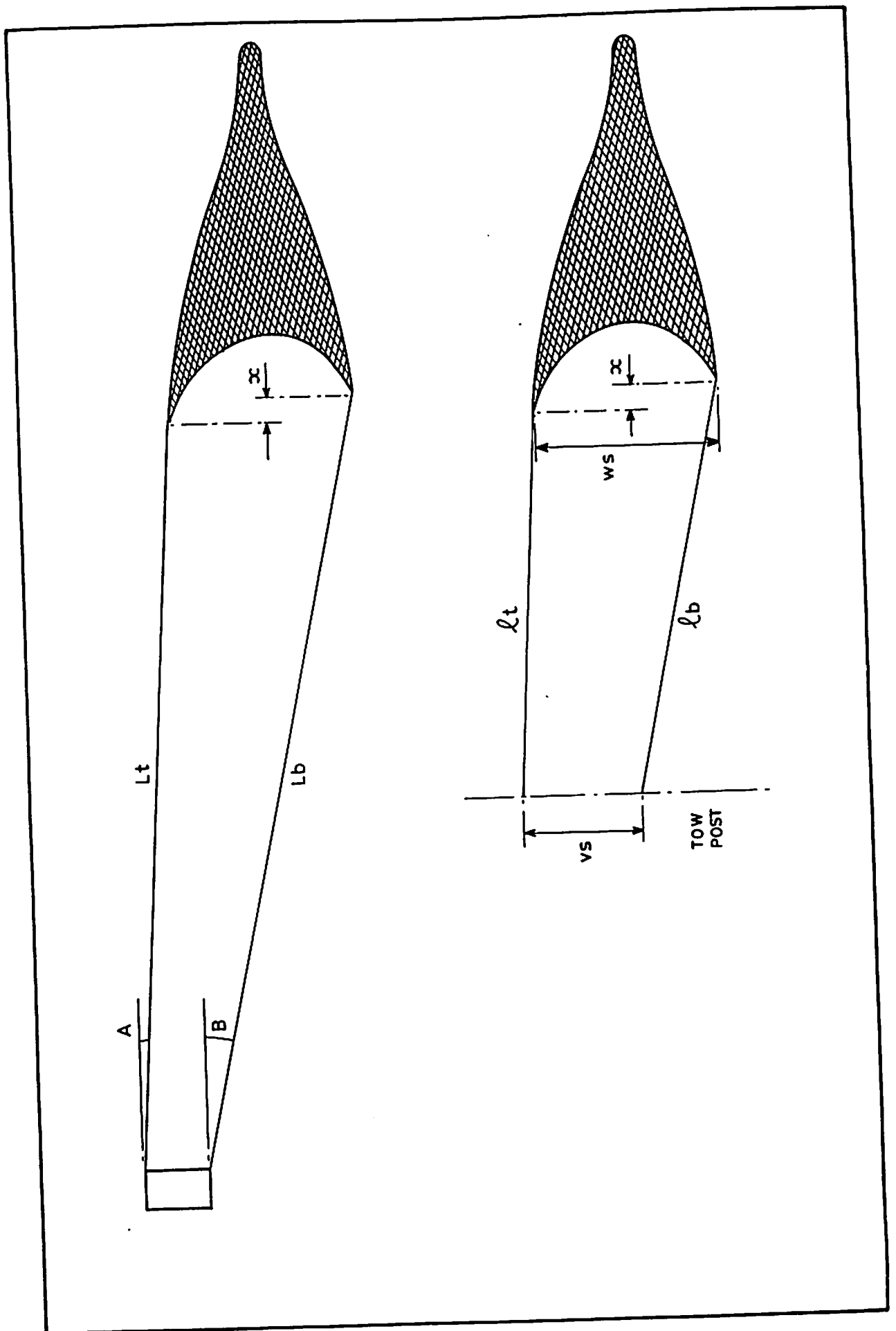


Fig.3 CALCULATION OF BRIDLE VERTICAL SEPARATION IN FLUME TANK

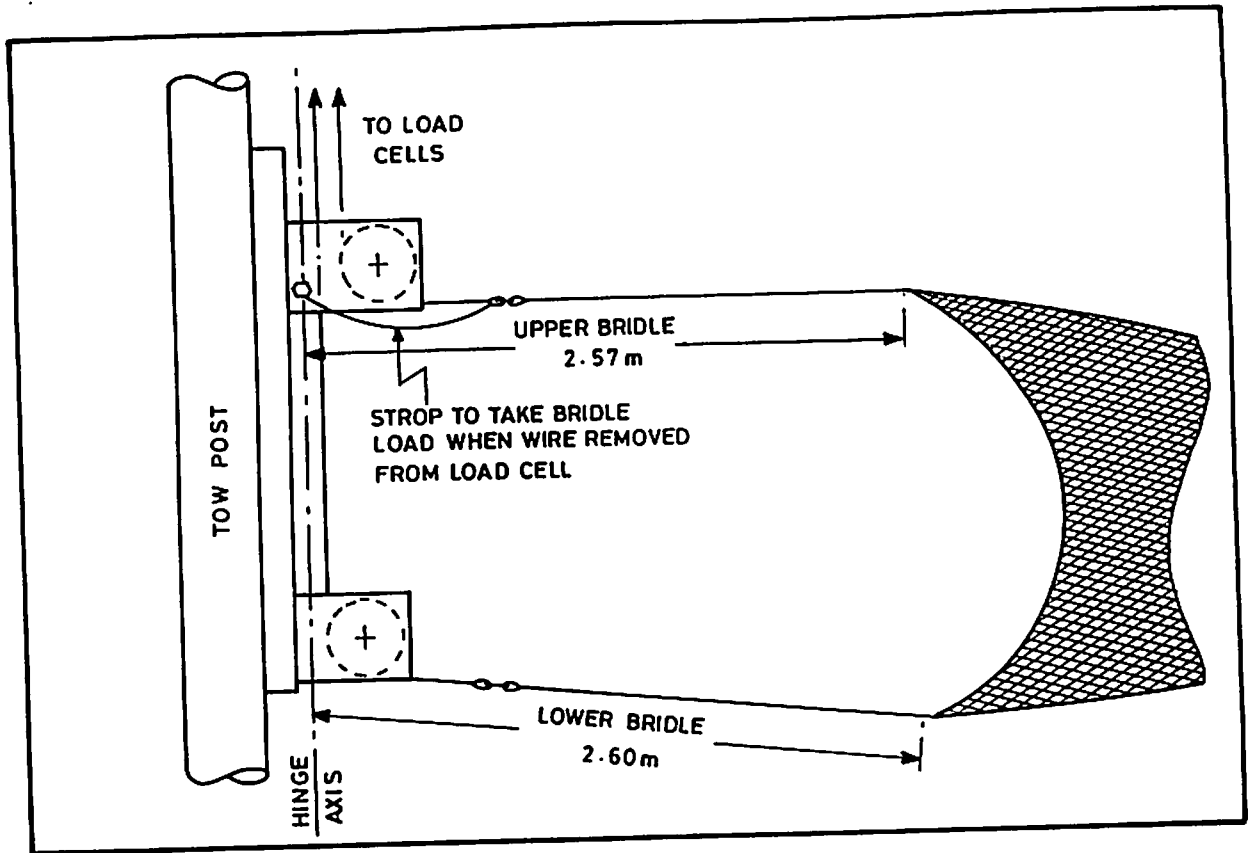


Fig.4 ATTACHMENT OF UPPER AND LOWER BRIDLES TO TOW POSTS

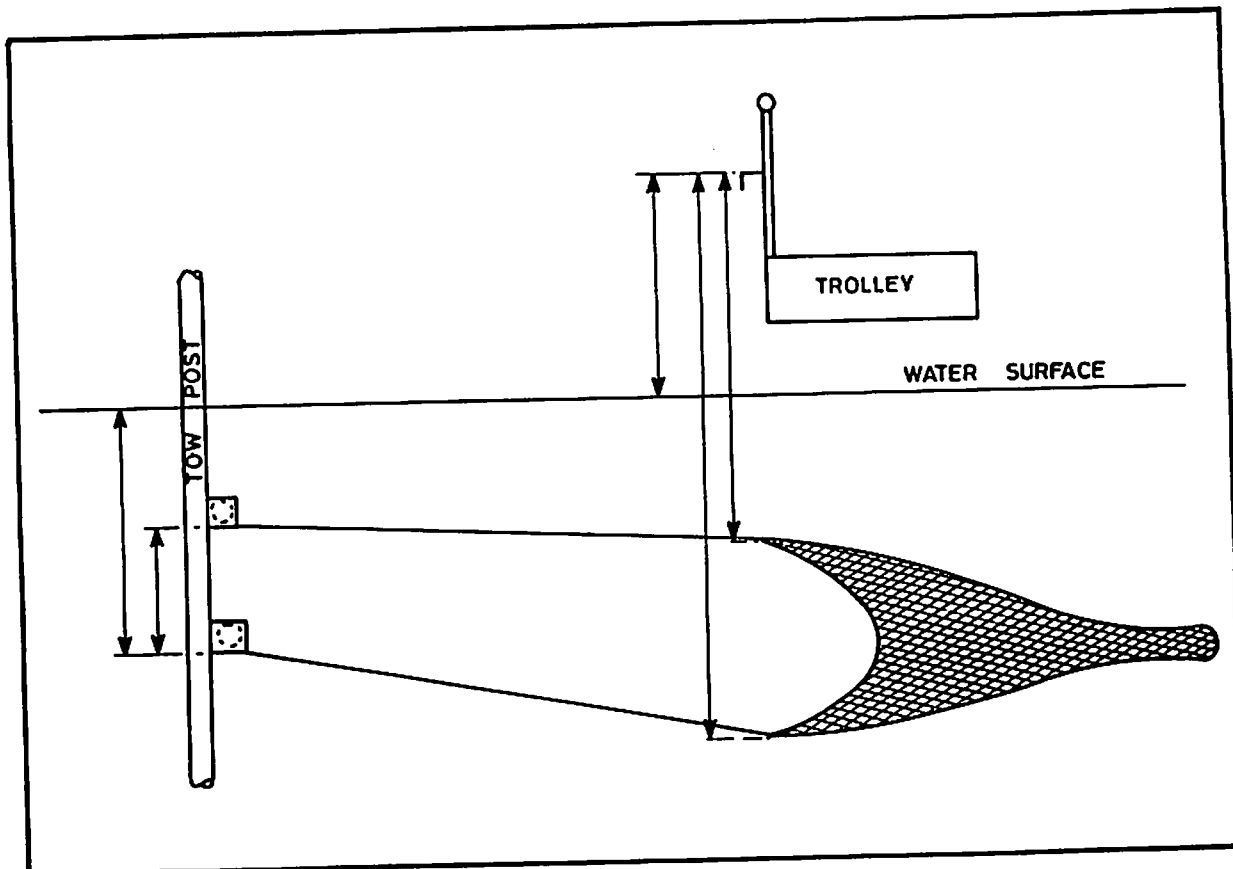


Fig.5 MEASUREMENT OF NET AND BRIDLES BELOW WATER SURFACE